

Superbunching from coherently driven atoms in a waveguide

Zeidan Zeidan,^{1,*} Therese Karmstrand,^{1,2} Maryam Khanahmadi,¹ and Göran Johansson¹

¹*Department of Microtechnology and Nanoscience (MC2), Chalmers University of Technology, 41296 Gothenburg, Sweden*

²*Theoretical Quantum Physics Laboratory, RIKEN Cluster for Pioneering Research, Wako-shi, Saitama 351-0198, Japan*

(Dated: June 6, 2025)

We investigate the scattered field from N identical two-level atoms resonantly driven by a weak coherent field in a one-dimensional waveguide. For atoms separated by the drive wavelength, increasing the number of atoms progressively suppresses transmission while enhancing photon bunching. Transmission becomes a superbunched ($N + 1$)-photon scattering process that is predominantly incoherent. Remarkably, we find that this transmission is only possible through a process where all N atoms are excited, enabling heralded multi-photon state generation with applications in long-distance entanglement and quantum metrology.

Introduction—Nonlinear light-matter interactions have been studied for decades, leading to the discovery of various quantum phenomena including nonclassical light state generation [1, 2], antibunching [2, 3], and superradiance [2, 4–6]. Multi-photon states, in particular, enable applications in quantum metrology [7–9], entanglement generation for quantum communication [10, 11], and quantum lithography [12, 13].

Waveguide quantum electrodynamics (wQED) has shown to be a promising platform for light-matter interactions due to the strong coupling between atoms and electromagnetic fields propagating in a one-dimensional waveguide. Experimentally, wQED has been demonstrated on various platforms [2, 14], including single-mode nanofibers coupled to cold atoms [15, 16], quantum dots in photonic crystals [17], and superconducting circuits [18–23].

It is well known that an atom in a waveguide almost perfectly reflects a weak resonant drive, and that the transmitted field is strongly bunched [14, 18, 20–22, 24–29]. For a single atom, the bunching occurs, somewhat counterintuitively, because a transmission event predominantly heralds the excitation of the atom [29], which then spontaneously emits a second photon. While this single-atom picture is well established, its extension to two or more atoms in the waveguide remains unexplored.

In this Letter, we study the scattering of a resonant coherent state by N atoms in a waveguide and demonstrate that, when driving weakly, increasing the number of atoms progressively suppresses the transmission while enhancing photon bunching. By considering atoms separated by the resonant wavelength, we derive exact analytical expressions describing the scattering dynamics. We find that transmission in the weak-drive regime is a superbunched ($N + 1$)-photon scattering process that is predominantly incoherent, with no phase relation to the drive. Remarkably, we analytically find that this transmission is only possible through a process where all N atoms are collectively excited. Thus, the first detection of a transmitted photon in a bunch heralds the atomic system most likely in a fully excited state. We verify our analytical findings with numerical simulations. Nat-

urally, this simple setup serves as an entanglement source and enables heralded multi-photon state generation with applications in quantum metrology.

Model—We consider N identical atoms spaced one radiation wavelength apart in a one-dimensional waveguide. The atoms are modeled as two-level systems with resonance frequency ω and are symmetrically coupled to the waveguide into which they decay through spontaneous emission with the rate γ to the left and right propagating fields (see Fig. 1). Neglecting the time delay between the closely spaced atoms, the master equation for the density matrix ρ of the atomic system, collectively and coherently driven with Rabi frequency Ω , is

$$\dot{\rho} = -i\frac{\Omega}{2}[S_+ + S_-, \rho] + \mathcal{D}(a_{\text{out}}^R)\rho + \mathcal{D}(a_{\text{out}}^L)\rho \quad (1)$$

where $\hbar = 1$, $\mathcal{D}(L)\rho = L\rho L^\dagger - \frac{1}{2}\{L^\dagger L, \rho\}$ is the Lindblad dissipator, $S_\pm = \sum_{i=1}^N S_\pm^i$ are the collective atomic dipole operators, and $a_{\text{out}}^{R/L}$ is the annihilation operator of the outgoing field propagating toward the right/left. The outgoing field operators are related to the annihilation operators of the incoming field from the right/left, $a_{\text{in}}^{R/L}$, through the input-output relations $a_{\text{out}}^L = a_{\text{in}}^R + \sqrt{\gamma}S_-$ and $a_{\text{out}}^R = a_{\text{in}}^L + \sqrt{\gamma}S_-$ [30, 31]. We consider an incoming coherent drive from the left with rate amplitude $\alpha = i\Omega/\sqrt{\gamma}$, and vacuum incoming from the right. When individual atomic relaxation and time delays are negligible, an atomic system initialized in the ground state evolves within the symmetric ($N + 1$)-dimensional Dicke subspace [4]. In the Hilbert space of the atomic system, the input-output relations then become $a_{\text{out}}^L = \sqrt{\gamma}S_-$ and $a_{\text{out}}^R = \alpha I_{N+1} + \sqrt{\gamma}S_-$, where I_{N+1} is the identity operator. Using the input-output relations, we can rewrite Eq. (1) as $\dot{\rho} = 2\mathcal{D}(a_{\text{out}}^R)\rho$, to immediately obtain the steady-state solution [34–39]:

$$\rho = \frac{(a_{\text{out}}^{R\dagger} a_{\text{out}}^R)^{-1}}{\text{Tr} (a_{\text{out}}^{R\dagger} a_{\text{out}}^R)^{-1}} = \frac{1}{D} \sum_{m,n=0}^N \left(\frac{S_-}{g^*} \right)^m \left(\frac{S_+}{g} \right)^n, \quad (2)$$

where the normalized drive amplitude $g = \alpha/\sqrt{\gamma} = i\Omega/\gamma$ and the normalization constant

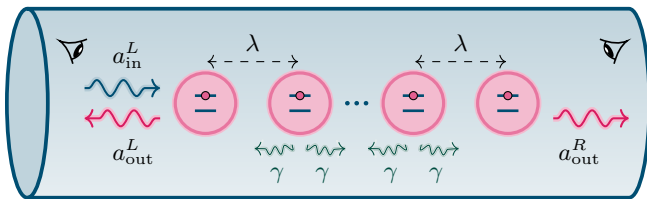


FIG. 1. N identical atoms, modeled as two-level systems, coupled to a waveguide. The atoms are spaced apart by wavelength distance λ and decay to the left and right propagating fields with spontaneous emission rate γ . The operator a_{in}^L refers to the annihilation operator of the incoming coherent drive from the left and $a_{\text{out}}^{R/L}$ is the operator of the outgoing field propagating toward the right/left. The eyes in the two corners represent photon detectors.

$D = \sum_{r=0}^N \binom{N+r+1}{2r+1} (r!)^2 |g|^{-2r}$. Using the steady-state solution from Eq. (2), we now calculate the scattered photon rates, providing initial insight into the system's dynamics and photon bunching behavior.

Scattered field—The average photon rate in the reflected and transmitted directions is given by $\bar{n}_{\text{ref}} = \langle a_{\text{out}}^{L\dagger} a_{\text{out}}^L \rangle$ and $\bar{n}_{\text{trans}} = \langle a_{\text{out}}^{R\dagger} a_{\text{out}}^R \rangle$, respectively. The scattered photon rate comprises phase-coherent components $\bar{n}_{\text{ref,coh}} = |\langle a_{\text{out}}^L \rangle|^2$ and $\bar{n}_{\text{trans,coh}} = |\langle a_{\text{out}}^R \rangle|^2$, with the remaining phase-incoherent components given by $\bar{n}_{\text{ref/trans,inc}} = \bar{n}_{\text{ref/trans}} - \bar{n}_{\text{ref/trans,coh}}$. The scattered phase-incoherent photons, attributed to spontaneous emission, are equal in the reflected and transmitted directions, $\bar{n}_{\text{ref,inc}} = \bar{n}_{\text{trans,inc}}$, due to the symmetry of emission into the waveguide. When weakly driven, $|g| \ll 1$, the atoms collectively oscillate coherently with a phase opposite to the input drive, leading to near-perfect reflection and effectively canceling the transmitted field [31], as in the single-atom case [14, 18, 20–22, 24–29]. Notably, in this regime, the transmission is predominantly incoherent and is given by [31]:

$$\bar{n}_{\text{trans}} \approx \bar{n}_{\text{trans,inc}} = \gamma |g|^{2(N+1)} \frac{N+1}{(N!)^2} + \mathcal{O}(|g|^{2(N+2)}), \quad (3)$$

which is proportional to the incoming rate of $(N+1)$ -photon states from the Poissonian drive. The scaling in Eq. (3) reveals that transmission requires driving the atomic system with sufficient photons to excite all N atoms. This behavior can be understood through two perspectives: (1) N atoms can coherently reflect Fock states of up to N photons, while states with $N+1$ or more photons enable incoherent transmission. (2) Although the average drive amplitude is in the linear regime, amplitude fluctuations occasionally probe the atomic non-linearity.

Moreover, in the weak-drive regime, the probability density for simultaneous detection of n transmitted photons is proportional to the zero-time n -th order correla-

tion function [31]:

$$G_{\text{trans}}^{(n)}(0) = \begin{cases} \gamma^n |g|^{2(N+1)} \binom{N+n}{2n-1} \left[\frac{(n-1)!}{N!} \right]^2 & \text{if } n \leq N, \\ \gamma^n |g|^{2n} \binom{n-1}{N}^2 & \text{if } n > N. \end{cases} \quad (4)$$

For $n \leq N+1$, $G_{\text{trans}}^{(n)}(0)$ scales as $|g|^{2(N+1)}$, matching the probability density of simultaneously detecting $N+1$ photons from the drive. In contrast, for $n > N+1$, the n -th order correlation function of both the transmitted field and input drive scale as $|g|^{2n}$. This scaling highlights that transmission is a process unlocked by at least $N+1$ input photons from the drive. While transmission events are rare in the weak driving regime, the second-order coherence function $g_{\text{trans}}^{(2)}(0) \propto |g|^{-2(N+1)} \gg 1$ reveals superbunched [24] transmission when it occurs. To further understand this $(N+1)$ -photon transmission process, we next examine the atomic system's quantum state conditioned on transmission.

Conditional atomic state—When conditioning the steady state from Eq. (2) on detecting a transmitted photon, we obtain the maximally mixed state

$$\rho_c = \frac{a_{\text{out}}^R \rho a_{\text{out}}^{R\dagger}}{\langle a_{\text{out}}^{R\dagger} a_{\text{out}}^R \rangle} = \frac{I_{N+1}}{N+1}. \quad (5)$$

In the strong driving regime, $|g| \gg 1$, the conditional state in Eq. (5), to leading order, coincides with the steady state in Eq. (2), as the drive saturates the atomic system and photon detections have a negligible effect on the state. However, the conditional state in Eq. (5) is *independent* of the normalized drive amplitude g . This raises the question of how to understand this state in the weak driving regime, $|g| \ll 1$, where the steady state is close to the ground state. In this regime, while the probability of detecting a transmitted photon is small, proportional to $|g|^{2(N+1)}$, when such a photon is detected, Eq. (5) tells us that the atomic system has an average of $N/2$ excitations. This can be understood by highlighting the fact that we are conditioning on detecting *any* transmitted photon. Transmission only occurs in bunches, as seen from Eqs. (3) and (4), following the collective excitation of all atoms, and each photon in the bunch could have been emitted from any excitation level of the system. This lack of information about which excitation level the transmitted photon was emitted from leads to maximal uncertainty in the atomic state.

To determine the atomic state after a specific transmitted click, we turn to the normalized no-click master equation, a master equation with removed jump/click terms [31, 40–42]. In the weak driving regime, the photon scattering rate is small, justifying the study of the no-click master equation. First, we consider the evolution described in Eq. (1) without transmitted clicks by removing the term $a_{\text{out}}^R \rho a_{\text{out}}^{R\dagger}$. When we condition the steady state of this no-click evolution on an inevitable

transmitted detection, we obtain the atomic state after the *first* transmitted click in a photon bunch. Using $|k\rangle_{\text{ex}}$ to denote the state with k excited atoms, this first-click state is given by [31]:

$$\rho_c^{\text{first}} = \sum_{k=0}^N \frac{1}{2^{N-k}(2-2^{-N})} |k\rangle\langle k|_{\text{ex}}. \quad (6)$$

Notably, the state in Eq. (6) follows an N -truncated geometric distribution, arising from the possibility of $N-k$ reflected photons preceding the first transmitted photon. This distribution is consistent with all incoherent scattering events involving $N+1$ photons, each having an equal $1/2$ probability of transmission or reflection. The highest probability corresponds to the fully excited state, i.e., $k=N$, occurring when the first photon is transmitted, and decreases by half with each additional previously reflected photon. The geometric distribution reveals that transmission originates from the fully excited state. We thus consider Eq. (1) without both reflected and transmitted clicks by removing the jump terms $a_{\text{out}}^L \rho a_{\text{out}}^{L\dagger}$ and $a_{\text{out}}^R \rho a_{\text{out}}^{R\dagger}$. Indeed, conditioning the steady state of this no-click evolution on an inevitable transmitted detection yields the fully excited atomic state $|N\rangle_{\text{ex}}$, confirming that transmission occurs through a process where all N atoms are excited.

Timescales—Having established that transmission is a multi-photon process, enabled when $(N+1)$ or more photons scatter off the atoms, we now make this picture more quantitative by defining the timescale T_{in} within which these photons must arrive to enable this transmission. In the weak-drive regime, transmission is dominated by the incoming rate of $N+1$ photons, as shown in Eq. (3). Incoming photons follow a Poisson distribution, and under weak driving, the probability of $N+1$ photons arriving within time T_{in} is $(\gamma|g|^2 T_{\text{in}})^{N+1}/(N+1)!$. These incoming photons yield $(N+1)/2$ transmitted photons, as they can either be reflected or transmitted, resulting in an average transmission rate of $(\gamma|g|^2)^{N+1} T_{\text{in}}^N/(2N!)$ [31]. By equating this rate with the transmission rate from Eq. (3), we arrive at

$$T_{\text{in}} = \frac{1}{\gamma} \left(\frac{2(N+1)}{N!} \right)^{1/N}. \quad (7)$$

Eq. (7) shows that, with increasing N , more input photons are required within a shorter time frame to trigger transmission. For large N , T_{in} is lower-bounded by $e/(\gamma N)$, qualitatively agreeing with the increasing collective coupling of the atomic system.

The second relevant timescale, T_{out} , characterizes the relaxation of an excited atomic state. From the fully excited state $|N\rangle_{\text{ex}}$, the atomic system undergoes cascaded emission from $|k\rangle_{\text{ex}}$ to $|k-1\rangle_{\text{ex}}$ at rates $\Gamma_k = 2\gamma \langle k|S_+ S_-|k\rangle_{\text{ex}} = 2\gamma(N-k+1)k$, until reaching the ground state $|0\rangle_{\text{ex}}$. This process forms a continuous-time absorbing Markov chain with $N+1$ states, where

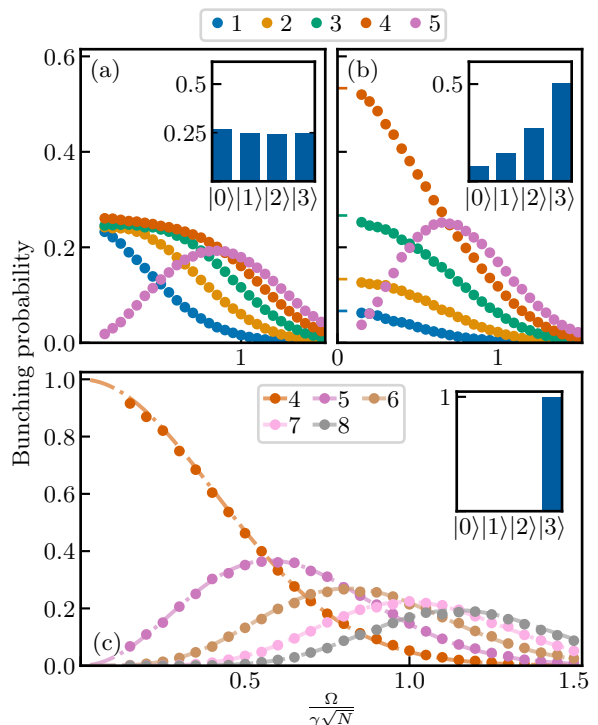


FIG. 2. Bunching probability versus effective drive amplitude $\Omega/(\gamma\sqrt{N})$, with $N=3$ atoms, $\gamma=1$, $T_{\text{in}}=1.10$ according to Eq. (7), and $T_{\text{out}}=T_{\text{out},99\%}=1.30$. The circles show simulation results, and different colors represent different photon bunch sizes. The insets display the average atomic state populations, conditioned on the first transmitted click, for the simulations with the weakest drive strength. For stronger drive strengths, the probabilities sum to less than one as the curves for larger-sized bunches are omitted. (a) All transmitted photons are counted as first clicks, i.e., clicks are re-counted. (b) The first transmitted click is defined as a transmitted detection preceded by no other transmitted photons during the time T_{in} . (c) The first transmitted click is defined as a transmitted detection preceded by neither transmitted nor reflected photons during the time T_{in} . The dash-dotted lines represent analytical predictions from Eq. (8) with the fitted timescales $\hat{T}_{\text{in}}=0.37$ and $\hat{T}_{\text{out}}=0.93$.

decay times between adjacent states follow exponential distributions with rates Γ_k . The total relaxation time follows a hypoexponential distribution [43–45], which is the sum of independent exponential random variables, with rate parameters $\Gamma_N, \dots, \Gamma_1$. Crucially, this statistical framework enables calculation of the p -th relaxation time quantile, $T_{\text{out},p}$, defined as the time by which the atomic system reaches the ground state with probability p . Additionally, the average relaxation time [5, 31] is given by $T_{\text{out,avg}} = \sum_{k=1}^N \frac{1}{\Gamma_k} = \frac{H_N}{\gamma(N+1)}$, where H_N is the N -th Harmonic number. The asymptotic limit for large N is $\ln(N)/(\gamma N)$, characteristic of superradiant collective spontaneous emission [5]. With these timescales established, we now turn to photon detection statistics obtained by numerical simulations.

Photon detection statistics—The master equation in Eq. (1) is simulated using Monte Carlo trajectory evolution [40, 46], with the output operators $a_{\text{out}}^{R/L}$ corresponding to photon detection in the transmitted and reflected fields according to Fig. 1. Here we present results for $N = 3$ atoms, while results for $N = 1$ and 2 atoms can be found in the End Matter. For our analysis, a photon bunch is defined by the number of clicks in the reflected and transmitted fields within a bunching time T_{out} after, and including, the first transmitted click. Fig. 2 shows the probability of obtaining a photon bunch of a given size versus the effective drive amplitude $\Omega/(\gamma\sqrt{N})$, demonstrating that different definitions of the *first transmitted click* yield different photon bunching statistics.

In Fig. 2(a), we employ a simple counting method where every transmitted photon is treated as a first click, effectively recounting photons that belong to the same bunching event. In the weak-drive regime we detect the mixed state as predicted in Eq. (5), however, for larger drive strengths most of the detected photons originate directly from the coherent drive and bunches typically contain more than five photons. In Fig. 2(b), we instead define the first transmitted click as a transmitted detection preceded by no other transmitted photons within the characteristic timescale T_{in} . In the weak-drive regime, the bunching probabilities approach the truncated geometric distribution, as predicted in Eq. (6).

In Fig. 2(c), we define the first transmitted click as a transmitted detection preceded by neither transmitted nor reflected photons during the time T_{in} . In the weak-drive regime, we approach exclusively $(N + 1)$ -photon bunches, as predicted by the no-click master equation. The analytical prediction for a k -photon bunch probability [31], plotted in Fig. 2(c), is given by

$$p(k) = \sum_{i=0}^{k-N-1} \Pr(Y = k - i) \Pr(Z = i), \quad (8)$$

where $k \geq N + 1$. The random variable Y , representing the initial photons that trigger transmission, follows an N -truncated Poisson distribution, while Z , accounting for additional input photons arriving during the emission process, follows a Poisson distribution. The summation in Eq. (8) captures all possible combinations of initial and additional photons that result in a k -photon bunch. For example, an $(N + 2)$ -photon bunch arises from either $N + 2$ initial photons with no additional arrivals, or $N + 1$ initial photons plus one additional arrival. The random variables Y and Z have the parameters $|\alpha|^2 \hat{T}_{\text{in}}$ and $|\alpha|^2 \hat{T}_{\text{out}}$, respectively, where the timescales \hat{T}_{in} and \hat{T}_{out} are obtained by fitting Eq. (8) to the simulation data. Interestingly, while these fitted timescales are systematically found to be shorter than those used to define photon bunches in the simulations [31], the analytical prediction of Eq. (8), nonetheless, shows excellent agreement with the numerical data in Fig. 2(c), even at intermediate and

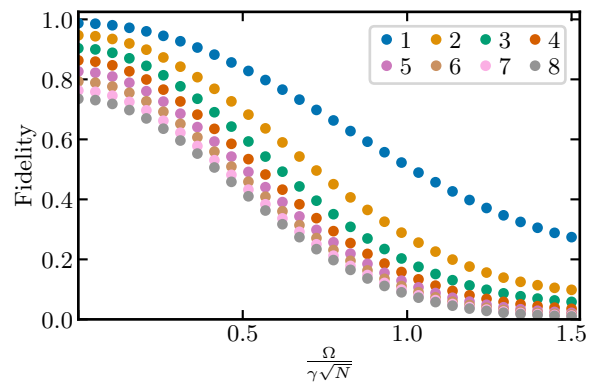


FIG. 3. Fidelity of the output field with the entangled binomial state, versus effective drive amplitude $\Omega/(\gamma\sqrt{N})$, for a system of initially fully excited atoms, for $N = 1$ to 8 atoms, represented by different colored markers, and $\gamma = 1$. The output states are taken at time $T_{\text{out},99\%}$.

strong drive. In the weak driving regime, the probability of obtaining an $(N + 1)$ -photon bunch from Eq. (8) can be approximated by $p(N + 1) = e^{-\Omega^2 T/\gamma}$, showing an exponential convergence to $(N + 1)$ -photon bunches [31].

Applications—Naturally, our simple setup enables multi-photon state generation and entanglement distribution, heralded by the detection of the first transmitted photon. Specifically, the bidirectional spontaneous emission from fully excited atoms produces an entangled binomial state, $|\psi_b\rangle = \sum_{k=0}^N \left[\binom{N}{k} 2^{-N} \right]^{1/2} |k, N - k\rangle_{L,R}$, between the left and right propagating modes. Fig. 3 shows the fidelity $\langle \psi_b | \rho_{\text{out}} | \psi_b \rangle$ between the output state ρ_{out} and the binomial state versus the effective drive amplitude $\Omega/(\gamma\sqrt{N})$ for up to eight atoms. Following [47, 48], we catch the output state by filtering with the optimal output mode shape corresponding to fully excited atoms decaying without drive. As shown in Fig. 3, the fidelity decreases with increased drive amplitude, as atomic emission is superposed with the coherent drive. Furthermore, lower fidelities correspond to higher atom numbers, as nonlinear decay generates multimode output states [48]. However, the optimal mode nevertheless captures at least 90% of the output photons for up to eight atoms [8]. Moreover, placing a mirror at an appropriate distance from the atoms in the transmitted direction [49] channels all N photons to propagate in a single direction. This enables applications in quantum metrology for quantum-enhanced phase measurements [7–9] and quantum lithography to beat the diffraction limit [12, 13].

Discussion—In summary, we have demonstrated that coherently driven atoms in a waveguide generate superbunched light, with the first transmitted photon heralding the atoms in a fully excited state. In a wider

scope, by applying the no-click master equation, we reveal the multi-photon emission mechanisms enabling heralded multi-photon state generation. While we study an arbitrary number of atoms, we note that the effects of the Markov approximation on photon bunching warrant investigation in future work. Finally, as we envision experimental implementation on superconducting waveguides, we plan to extend this work to transmon systems while studying how anharmonicity, dephasing, and detuning affect the photon bunching robustness.

Acknowledgements—We thank I. Lyngfelt and B. Bertin-Johannet for feedback on the manuscript. We acknowledge support from the Knut and Alice Wallenberg Foundation through the Wallenberg Centre for Quantum Technology (WACQT). Z. Z. and G. J. acknowledge support from the Swedish Research Council, grant no. 2021-04037. T. K. acknowledges support from the FY2024 JSPS Postdoctoral Fellowship for Research in Japan. The simulations were enabled by resources provided by the National Academic Infrastructure for Supercomputing in Sweden (NAISS), partially funded by the Swedish Research Council through grant no. 2022-06725.

* zeidan.zeidan@chalmers.se

- [1] N. V. Corzo, J. Raskop, A. Chandra, A. S. Sheremet, B. Gouraud, and J. Laurat, *Nature* **566**, 359–362 (2019).
- [2] A. S. Sheremet, M. I. Petrov, I. V. Iorsh, A. V. Poshakinskiy, and A. N. Poddubny, *Reviews of Modern Physics* **95**, 015002 (2023).
- [3] A. S. Prasad, J. Hinney, S. Mahmoodian, K. Hammerer, S. Rind, P. Schneeweiss, A. S. Sørensen, J. Volz, and A. Rauschenbeutel, *Nature Photonics* **14**, 719–722 (2020).
- [4] R. H. Dicke, *Physical Review* **93**, 99–110 (1954).
- [5] M. Gross and S. Haroche, *Physics Reports* **93**, 301–396 (1982).
- [6] A. Goban, C.-L. Hung, J. Hood, S.-P. Yu, J. Muniz, O. Painter, and H. Kimble, *Physical Review Letters* **115**, 063601 (2015).
- [7] V. Paulisch, M. Perarnau-Llobet, A. González-Tudela, and J. I. Cirac, *Physical Review A* **99**, 043807 (2019).
- [8] M. Perarnau-Llobet, A. González-Tudela, and J. I. Cirac, *Quantum Science and Technology* **5**, 025003 (2020).
- [9] M. Khanahmadi and K. Mølmer, *Physical Review A* **107**, 013705 (2023).
- [10] B. Blauensteiner, I. Herbauts, S. Bettelli, A. Poppe, and H. Hübel, *Phys. Rev. A* **79**, 063846 (2009).
- [11] M. Maffei, D. Pomarico, P. Facchi, G. Magnifico, S. Pascazio, and F. V. Pepe, *Phys. Rev. Res.* **6**, L032017 (2024).
- [12] A. N. Boto, P. Kok, D. S. Abrams, S. L. Braunstein, C. P. Williams, and J. P. Dowling, *Physical Review Letters* **85**, 2733–2736 (2000).
- [13] G. Björk, L. L. Sánchez-Soto, and J. Söderholm, *Physical Review Letters* **86**, 4516–4519 (2001).
- [14] D. E. Chang, A. S. Sørensen, E. A. Demler, and M. D. Lukin, *Nature Physics* **3**, 807–812 (2007).
- [15] E. Vetsch, D. Reitz, G. Sagué, R. Schmidt, S. T. Dawkins, and A. Rauschenbeutel, *Phys. Rev. Lett.* **104**, 203603 (2010).
- [16] R. Pennetta, M. Blaha, A. Johnson, D. Lechner, P. Schneeweiss, J. Volz, and A. Rauschenbeutel, *Physical Review Letters* **128**, 073601 (2022).
- [17] P. Lodahl, A. Floris van Driel, I. S. Nikolaev, A. Irman, K. Overgaag, D. Vanmaekelbergh, and W. L. Vos, *Nature* **430**, 654–657 (2004).
- [18] O. Astafiev, A. M. Zagoskin, A. A. Abdumalikov, Y. A. Pashkin, T. Yamamoto, K. Inomata, Y. Nakamura, and J. S. Tsai, *Science* **327**, 840–843 (2010).
- [19] A. A. Abdumalikov, O. Astafiev, A. M. Zagoskin, Y. A. Pashkin, Y. Nakamura, and J. S. Tsai, *Physical Review Letters* **104**, 193601 (2010).
- [20] I.-C. Hoi, C. M. Wilson, G. Johansson, T. Palomaki, B. Peropadre, and P. Delsing, *Physical Review Letters* **107**, 073601 (2011).
- [21] I.-C. Hoi, T. Palomaki, J. Lindkvist, G. Johansson, P. Delsing, and C. M. Wilson, *Physical Review Letters* **108**, 263601 (2012).
- [22] I.-C. Hoi, C. M. Wilson, G. Johansson, J. Lindkvist, B. Peropadre, T. Palomaki, and P. Delsing, *New Journal of Physics* **15**, 025011 (2013).
- [23] A. F. van Loo, A. Fedorov, K. Lalumière, B. C. Sanders, A. Blais, and A. Wallraff, *Science* **342**, 1494–1496 (2013).
- [24] Z. Ficek and S. Swain, *Quantum Interference and Coherence* (Springer-Verlag, 2005).
- [25] J. T. Shen and S. Fan, *Optics Letters* **30**, 2001 (2005).
- [26] J.-T. Shen and S. Fan, *Phys. Rev. Lett.* **95**, 213001 (2005).
- [27] H. Zheng, D. J. Gauthier, and H. U. Baranger, *Physical Review A* **82**, 063816 (2010).
- [28] B. Peropadre, J. Lindkvist, I.-C. Hoi, C. M. Wilson, J. J. Garcia-Ripoll, P. Delsing, and G. Johansson, *New Journal of Physics* **15**, 035009 (2013).
- [29] X. H. H. Zhang and H. U. Baranger, *Physical Review A* **97**, 023813 (2018).
- [30] K. Lalumière, B. C. Sanders, A. F. van Loo, A. Fedorov, A. Wallraff, and A. Blais, *Physical Review A* **88**, 043806 (2013).
- [31] See Supplemental Material at URL-inserted-by-publisher for lengthier derivations, which includes Refs. [32–33].
- [32] J. Riordan, *Combinatorial Identities*, 99th ed., Wiley series in probability and mathematical statistics (John Wiley & Sons, Nashville, TN, 1968).
- [33] M. Mitzenmacher and E. Upfal, *Probability and Computing: Randomized Algorithms and Probabilistic Analysis* (Cambridge University Press, 2005).
- [34] R. R. Puri and S. V. Lawande, *Physics Letters A* **72**, 200–202 (1979).
- [35] R. Puri and S. Lawande, *Physica A: Statistical Mechanics and its Applications* **101**, 599–612 (1980).
- [36] P. D. Drummond, *Phys. Rev. A* **22**, 1179 (1980).
- [37] S. V. Lawande, R. R. Puri, and S. S. Hassan, *Journal of Physics B: Atomic and Molecular Physics* **14**, 4171–4189 (1981).
- [38] S. Hassan, R. Bullough, R. Puri, and S. Lawande, *Physica A: Statistical Mechanics and its Applications* **103**, 213–225 (1980).
- [39] S. S. Hassan, G. P. Hildred, R. R. Puri, and R. K. Bullough, *Journal of Physics B: Atomic and Molecular Physics* **15**, 2635–2655 (1982).
- [40] K. Mølmer, Y. Castin, and J. Dalibard, *Journal of the Optical Society of America B* **10**, 524 (1993).

- [41] H.-P. Breuer and F. Petruccione, *The Theory of Open Quantum Systems* (Oxford University Press, 2007).
- [42] H. M. Wiseman and G. J. Milburn, *Quantum Measurement and Control* (Cambridge University Press, 2009).
- [43] S. Amari and R. Misra, *IEEE Transactions on Reliability* **46**, 519–522 (1997).
- [44] G. Bolch, S. Greiner, H. de Meer, and K. S. Trivedi, *Queueing Networks and Markov Chains: Modeling and Performance Evaluation With Computer Science Applications* (Wiley, 2006).
- [45] B. Legros and O. Jouini, *Applied Mathematical Modelling* **39**, 4971–4977 (2015).
- [46] N. Lambert, E. Giguère, P. Menczel, B. Li, P. Hopf, G. Suárez, M. Gali, J. Lishman, R. Gadhvi, R. Agarwal, A. Galicia, N. Shammah, P. Nation, J. R. Johansson, S. Ahmed, S. Cross, A. Pitchford, and F. Nori, *Qutip 5: The quantum toolbox in python* (2024).
- [47] A. H. Kñilerich and K. Mølmer, *Phys. Rev. Lett.* **123**, 123604 (2019).
- [48] M. Khanahmadi, M. M. Lund, K. Mølmer, and G. Johansson, *Physical Review Research* **5**, 043071 (2023).
- [49] S. R. Sathyamoorthy, A. Bengtsson, S. Bens, M. Simoen, P. Delsing, and G. Johansson, *Phys. Rev. A* **93**, 063823 (2016).

End Matter

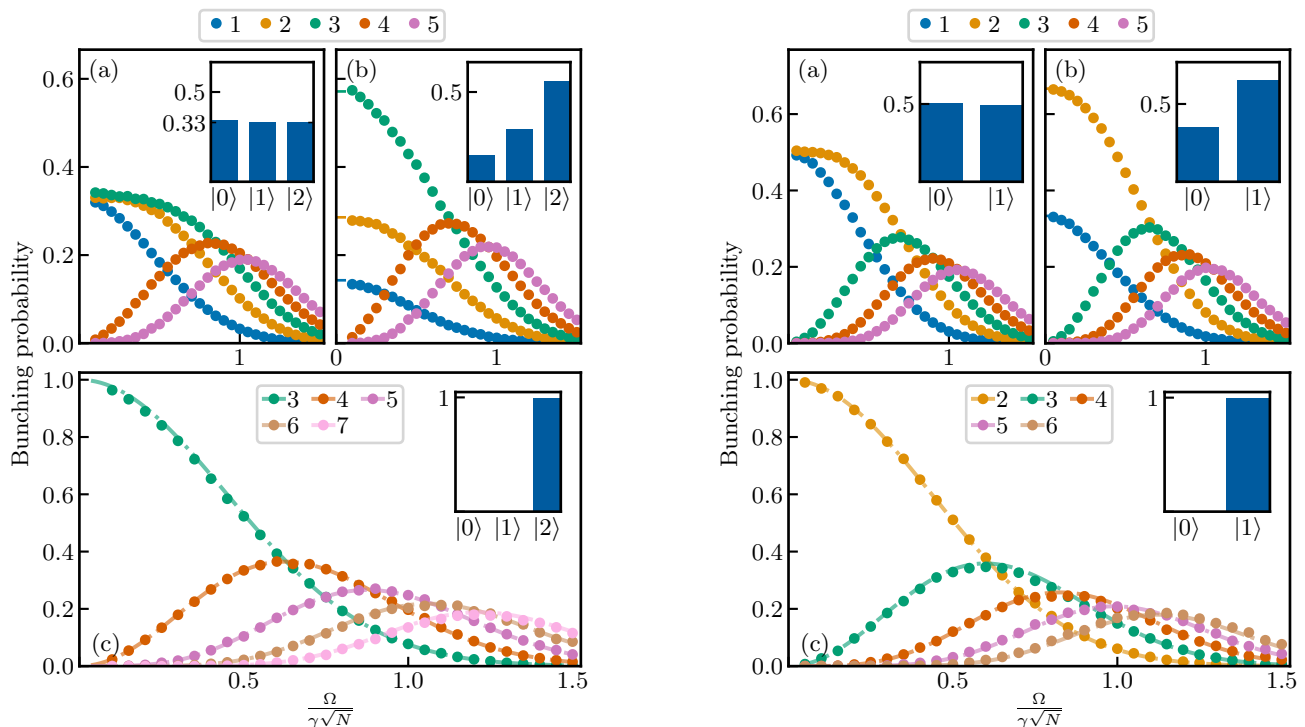


FIG. 4. Bunching probability versus effective drive amplitude $\Omega/(\gamma\sqrt{N})$. The left (right) panel corresponds to $N = 2$ (1) atoms, with the simulation parameters $\gamma = 1$, $T_{in} = 1.70$, $T_{out} = T_{out,99\%} = 1.66$, and $\gamma = 1$, $T_{in} = 4$, $T_{out} = T_{out,99.9\%} = 3.45$, respectively. The circles show simulation results, and different colors represent different photon bunch sizes. The insets display the average atomic state populations, conditioned on the first transmitted click, for the simulations with the weakest drive strength. For stronger drive strengths, the probabilities sum to less than one as the curves for larger-sized bunches are omitted. (a) All transmitted photons are counted as first clicks, i.e., clicks are recounted. (b) The first transmitted click is defined as a transmitted detection preceded by no other transmitted photons during the time T_{in} . (c) The first transmitted click is defined as a transmitted detection preceded by neither transmitted nor reflected photons during the time T_{in} . The dash-dotted lines represent analytical predictions from Eq. (8) with the fitted timescales $\hat{T}_{in} = 0.83$, and $\hat{T}_{out} = 1.05$ for the left panel, and $\hat{T}_{in} = 2.58$, and $\hat{T}_{out} = 1.80$ for the right panel.